Received: 7 March 2022 | Revised: 2 May 2022 | Accepted: 24 May 2022

DOI: 10.1002/rcs.2428

ORIGINAL ARTICLE

The International Journal of Medical Robotics and Computer Assisted Surgery

WILEY

An admittance-controlled amplified force tracking scheme for collaborative lumbar puncture surgical robot system

Hongbing Li[1] | Xun Nie[2] | Ding Duan[2] | Yuling Li[2] | Jing Zhang[3] | Min Zhou[3] | Evgeni Magid[4,5]

[1]Department of Instrument Science and Engineering, and Shanghai Engineering Research Center for Intelligent Diagnosis and Treatment Instrument, School of Electronic Information and Electrical Engineering, Shanghai Jiao Tong University, Shanghai, China

[2]Department of Instrument Science and Engineering, School of Electronic Information and Electrical Engineering, Shanghai Jiao Tong University, Shanghai, China

[3]Department of Hematology and Oncology, Shanghai Children's Medical Center, Shanghai Jiao Tong University School of Medicine, Shanghai, China

[4]Institute of Information Technology and Intelligent Systems, Kazan Federal University, Kazan, Russia

[5]HSE University, Moscow, Russia

Correspondence
Hongbing Li, Department of Instrument Science and Engineering, and Shanghai Engineering Research Center for Intelligent Diagnosis and Treatment Instrument, School of Electronic Information and Electrical Engineering, Shanghai Jiao Tong University, Shanghai 200240, China.
Email: lihongbing@sjtu.edu.cn

Funding information
The Projects of the Shanghai Science and Technology Committee, Grant/Award Numbers: 21S31906100, 21S31903300, 22S31904100; Kazan Federal University Strategic Academic Leadership Program

Abstract

Background: The accurate sensing and display of the delicate needle-tissue interaction force to the operator is desirable for needle insertion procedures. It not only plays a significant role in the surgical treatment effect, but also has a great significance in improving surgical safety and reducing the incidence of complications. However, the direct detection of the interaction force between the tissue and needle tip by placement of a force sensor is challenging owing to the constraints of miniaturisation, cost, and sterilisation.

Methods: In this study, a new position-based force-to-motion controller with magnified force feedback is presented to provide augmented force perception to the operator during needle insertion on the soft tissue. Furthermore, the demonstration to the position-based low level motion controller is more suitable for needle insertion surgical requirements in the cooperative robotic system.

Results: The proposed controller was experimentally validated by a collaborative lumbar puncture robotics system. Additionally, to provide hand tremor rejection for the stable manipulation of the puncture needle, it was demonstrated that the proposed amplified feedback force controller allowed a safer object interaction with the robotic needle insertion assistance.

Conclusions: The results of the experiment show that a desirable interaction force profile is perceived by the operator during the overall insertion task operation. The admittance gain for the simplified admittance controller has a significant impact on the operator's ability to accurately control the applied force.

KEYWORDS
collaborative manipulation, force perception, lumbar puncture, needle insertion

1 | INTRODUCTION

ROBOTIC technology has been adopted rapidly in hospitals worldwide over the past decades. A wide range of surgical procedures are now performed by robot-assisted systems. The introduction of robotic technology both affects the patient's treatment outcomes and surgeon's manipulation experiences. Robot-assisted systems facilitate the performance of surgical procedures by enhancing the tool tip precision and reducing hand tremor during delicate surgery manoeuvres.[1] Because the autonomous surgical robot system is far from being approved for clinical use and replacing surgeons, most robot-assisted systems developed worldwide belong to non-autonomous systems.[2,3] Presently non-autonomous surgical robot systems can be classified into two categories, tele-manipulated and *collaborative*,

according to the distance between the patients and clinicians. The first group, master slave teleoperation configuration, executes specific surgical tasks to reproduce the remote or actual surgeon's hand motion with deep intervention of the practitioner. Currently, telemanipulation surgical robots have emerged as the most clinically ready configuration for minimally invasive surgery, such as the da Vinci surgical robot system.[4] *Collaborative or hands-on* robots, on the other hand, share the same working space and control of the surgical tool with the surgeon and aim to manually guide the surgical instruments the surgeon. In this context, the human operator drives the tool of the surgical robot towards the target by applying guiding forces and torques on a handle. Neither the tele-operated surgical robot system nor the collaborative robots are developed to replace the surgeon. Rather, they are intended to augment and improve the performance of medical staff during the execution of surgical tasks that would not otherwise be physically possible. However, both the tele-operated and cooperative surgical robot systems in clinical applications lack the delicate tool-tissue interaction force feedback to the operator. Advancements in the collaborative robot have potentially increased patient safety by reducing hand tremor and tool precision. Currently, the collaborative surgical robot system has attracted considerable attention in clinical applications.[5,6]

In conventional manual surgery, surgeons rely heavily on the visual and force feedback they attain when they are manipulating the surgical tool.[7,8] However, the dynamic interaction forces between the surgical tool and tissue are no longer perceived by the surgeon when complex robot systems are introduced to the procedure. For a collaborative surgical robot system, two effective control strategies, compliance control and the force feedback algorithm, are needed to guarantee the safe execution of surgical task. One of the main difficulties in delicate surgical tasks lies in controlling the cooperative manipulators complying with the physician.[9] In all surgical applications, it is paramount to reliably control the tool-tissue interaction forces within a safe range, where the surgeon still retains full control of the operation. To address the compliance issue in collaborative configuration, various control algorithms have been proposed in the literature.

Active compliance control methods, such as impedance and admittance control, are widely used in robot-assisted systems both in the medical community[10,11] and industrial applications.[12] Both control methods allow the implementation of a desired dynamic behaviour between external forces and the robot motion depending on the causality of the controller. An impedance robot-assisted system measures motion and displays force, whereas an admittance type robotic system measures force and displays motion.[9] One of the key features of such schemes is that the control transitions between the contact and non-contact is not required compared with the hybrid position-force control.

In recent years, admittance control has become a standard approach for physical human-robot interaction applications.[13–15] Collaborative robotic systems based on admittance control have been proved to be the most efficient control method in highly demanding surgical procedures. In Reference[16] a variable Cartesian impedance strategy based on the interpretation of the operator's intentions was proposed to ensure the best performance of the redundant robot. To enable stable and low effort manipulation on a robot, the admittance gains are adjusted online by the measurement of the environment stiffness.[17] To maintaining the system passivity, Landi et al.[18] presented a passivity-framework for adapting the parameters of the admittance control in physical human-robot interaction. In Sharkawy et al.[19] proposed a variable admittance controller for human-robot cooperation based on feedforward neural network training. To offer robust system stability and improve system transparency, a fractional order admittance controller was proposed by Aydin et al. in.[20] The experimental results showed that the operator manipulation effort could be reduced significantly. In Kang et al.[21] a variable admittance controller for physical human-robot interaction was proposed to achieve intuitive control of the robot based on operator intention recognition. A variable admittance controller is proposed in Bazzi et al.[22] to help the operator in directing the hand-guiding robot towards a predefined goal position.

Generally, a lower level closed-loop controller is required to set the system output on the reference input generated by the admittance controller in a human-robot cooperation system. Although the admittance control can improve the performance of the physical human-robot interaction, the method does not guarantee operational security in medical applications because it can only regulate the interaction force without constraining the end tool position of the surgical robot.[22,23] Consequently, the precise estimation of the position of the end tool inside the patient's tissue becomes difficult. Furthermore, for the traditional admittance-type collaborative surgical robot system, sensing the delicate tool-tissue interaction force by the operator from the handle of the assisted robot is almost impossible because the small force variations at the tool tip are masked by the relatively large friction force between the tool shaft and surrounding tissue.[24]

Based on the abovementioned discussion, in this article, a force augmentation algorithm and soft saturation function are jointly designed to guarantee the lumbar puncture robot end-effector within the constrained task space. An admittance-based controller for physical human-robot interaction is designed to solve the uncertainties in dynamics. Additionally, the proposed controller can guarantees the end-effector of the lumbar puncture robot in the constrained task space and improves the compliance of the robot-environment interaction. To the best of our knowledge, there is no report on a provably asymptotically stable delicate force amplification controller for robot-assisted needle insertion systems in previous literature. This study attempts to fill this lacuna by proposing a new puncture force augmentation controller for the collaborative surgical robot which guarantees exact force trajectory tracking under the position-based admittance controller. Compared with existing works, the main contributions of this paper include the following.

1) This study explicitly considers the scaling factor that describes the relationship between the human applied force of the end-effector and the corresponding tool-environment interaction

force, because many surgical applications that require a high degree of precision also require magnification of the workspace. Experiments are conducted to determine the effects of the admittance gain, velocity, and scale factor on human force control.

2) We prove that the velocity-control relative accuracy and precision both deteriorate as either the velocity or applied force become very low. The results will be valuable in the design of admittance-type surgical robot systems, particularly those implementing force gain scheduling, which aim to balance between precision and efficiency in medical applications.
3) We report that admittance gain is for the simplified admittance controller and has a significant influence on the operator's ability to precisely control the applied force. There is a tradeoff between the force control accuracy and operator's fatigue for optimal task performance.

The rest of the paper is organised as follows. Section 2 explains the preliminaries and problem formulation. Section 3 describes the control architecture of the cooperative surgical robot system. Section 4 presents the stability analysis of the admittance controlled system. Section 5 details the force amplification algorithm for the lumbar puncture robotic system. In Section 6, the applicability of the approach in a real manual guidance scenario and the analysis of the experimental results are presented. Section 7 concludes and summarises the results.

2 | PRELIMINARIES AND PROBLEM FORMULATION

2.1 | Problem formulation

For a collaborative surgical robot system in a constrained task space, the motion of the robot should comply well with the human operator input force, excessive interaction force between the human operator and manipulator should be avoided to reduce uncomfortable feelings for the operator. Additionally, safety during the collaborative surgical manipulation should be ensured to avoid unexpected damage to the target tissue. Our control objective is to design a controller for the surgical manipulator that can track the desired force profile and simultaneously guarantee that the desired admittance relationship of the surgical manipulator can be achieved under the proposed controller.

2.2 | System modelling of surgical robot

The collaborative lumbar puncture robot system was a four degree of freedom robot developed at the Shanghai Jiao Tong University for medical needle insertion applications.[25–28] The dynamic model of the surgical robot in the joint space is of the form:

$$M(q)\ddot{q} + C(q,\dot{q})\dot{q} + g(q) + \tau_f = \tau_c + J^T(q)f_{ext} \tag{1}$$

where $q \in \mathbb{R}^n$, with $n = 4$, is the vector of the joint variables, $\dot{q}, \ddot{q} \in \mathbb{R}^n$ are the velocity and acceleration of the joint angles, $M(q)$ denotes the inertia matrix, $C(q,\dot{q})\dot{q}$ is the vector of the Coriolis/centrifugal torques, $g(q)$ is the vector of the gravitational torques, τ_f is the vector of the joint friction torques, τ_c denotes the control input to the robot actuators, $J(q)$ is the robot Jacobian, and $\tau_{ext} = J^T(q)f_{ext}$ denotes the joint torque resulting from the external force and torque f_{ext} applied to the robot. Here, f_{ext} can be classified into two types, one is the external active applied force by the operator f_h, and the other is the passive applied external force from the interaction of the environment with the puncture needle f_n.

To design the admittance control algorithm, it is useful to derive the surgical robot dynamics in the operational space. To design a task-space control law, we first need the relationship between the joint angles $q \in \mathbb{R}^n$ and the end-effector position $x \in \mathbb{R}^m$ of the robotic system,

$$x = f(q), q = f^{-1}(x) \tag{2}$$

where $f(\cdot) : \mathbb{R}^n \to \mathbb{R}^m$ is the forward kinematics of the surgical robot, and $f^{-1}(\cdot) : \mathbb{R}^m \to \mathbb{R}^n$ is the inverse kinematics. Here, the inverse kinematics solution $f^{-1}(\cdot)$ of the surgical robot is feasible because the joint space degree of freedom is equal to the task space degree of freedom, that is $n = m$. The velocity kinematics is expressed as

$$\dot{x} = \frac{\partial f(q)}{\partial q}\dot{q} = J(q)\dot{q} \tag{3}$$

where $J(q) \in \mathbb{R}^{n\times m}$ denotes the Jacobian matrix in the robotic system. Based on inverse kinematics, the joint velocity$\dot{q}$ and acceleration $\ddot{q}$ can be calculated as follows:

$$\begin{cases} \dot{q} = J^{\dagger}(q)\dot{x} \\ \ddot{q} = \dot{J}^{\dagger}(q)\dot{x} + J^{\dagger}(q)\ddot{x} \end{cases} \tag{4}$$

where $x = [x_1, x_2, \ldots, x_n]^T$ is the position vector of the tool for the manipulator in the task space, and the Moore-Penrose pseudo inverse Jacobian matrix $J^{\dagger}$ is the dynamically consistent generalised inverse of kinematics $J(q)$, defined as:

$$J^{\dagger} = M^{-1}J^T\left(JM^{-1}J^T\right)^{-1} = J^T\left(JJ^T\right)^{-1} \tag{5}$$

Then substituting Equation (4) into dynamic model (Equation 1), the dynamics of the robot in the task space is obtained as follows:

$$\Lambda(q)\ddot{x} + \Psi(q,\dot{q})\dot{x} + f_g(q) + f_f(q) = f_c + f_{ext} \tag{6}$$

where $\Lambda(q) = J^{\dagger T}(q)M(q)J^{\dagger}(q)$ is the inertia matrix of the robot, hereafter denoted as the apparent inertia, where $\Psi\dot{x} = \Lambda\left(JM^{-1}C - \dot{J}\right)\dot{q}$, $f_g = J^{\dagger T}g$, $f_f = J^{\dagger T}\tau_f$ and $f_c = J^{\dagger T}\tau_c$ are the forces, reflected at the end-effector of the robot, corresponding to the non-inertial joint torques in (Equation 1).

3 | CONTROL ARCHITECTURE

In this collaborative lumbar puncture robotic system, we assume that there are physical interactions between the operator, surgical robot, and object environment. The human operator interacts with the surgical robot by moving the handle along arbitrary trajectories. During the cooperation condition, the operator applies a guiding force f_h through the handle to the surgical robot to move the needle of the lumbar puncture robot at a desired velocity $\dot{x}_r$. The guiding force f_h is measured by the force sensor fixed on the handle of the robot.

When the end-effector of the surgical robot interacts with the object, the resultant interaction force f_n is measured by a force sensor attached to the needle holder of the robot. This sensed guiding force signal is filtered by a low pass filter $H(s)$, and then sent to the admittance controller $Y(s)$ as the input signal. The control strategy is designed to perform tasks in cooperation with the operators. Generally, it is more natural to use admittance control when the robots are utilised in human hands-on guiding surgical tasks. The power transmission trains of such robotic systems often feature significant joint friction and are non-backdrivable.

In such a surgical robot system, it is assumed that only forces can be applied to the robot. The lower level motion controller of the lumbar puncture robot system is robust to the external interaction force from the environment acting on the needle tip and it is assumed that the movement of the surgical manipulator is not significantly affected by these external applied forces. The admittance control architecture implemented in this study is shown by Figure 1.

3.1 | Inner motion control loop

As shown by Figure 1, in the admittance control, the robot is motion-controlled and behaves as mechanical impedance. Practically, a lower level closed-loop motion controller is designed to set the robot system to track the reference input generated by the admittance controller. This lower level motion servo controller can be categorised into two types: velocity-based servo controller and position-based servo controller:

3.1.1 | Inner velocity-based servo control loop

This controller guarantees asymptotically exact position and velocity tracking for all position trajectories for the non-contact robot motion. The most commonly used inner velocity controller in literature includes the proportional or proportional-integral velocity control methods. Under an inner loop proportional velocity control law,

$$f_c = k_d \Delta \dot{x} \tag{7}$$

where $\Delta \dot{x}(t) = \dot{x}_r(t) - \dot{x}(t)$ is the velocity tracking error.

3.1.2 | Inner position-based servo control loop

The inner position closed control loop is used to follow a desired position and velocity. The position controller is more intuitive when considering the dynamic interaction between the robot end-effector and environment. The proportional-derivative control law is written as

$$f_c = k_p \Delta x + k_d \Delta \dot{x} \tag{8}$$

where $\Delta x(t) = x_r(t) - x(t)$ is the position tracking error.

3.2 | Outer force control loop

The second basic component of the admittance controller shown in Figure 1 is the transformation of the human guiding force into a desired position or velocity trajectories. In practice, two types of admittance controllers in the literature: simplified admittance controller, and normal admittance controller.

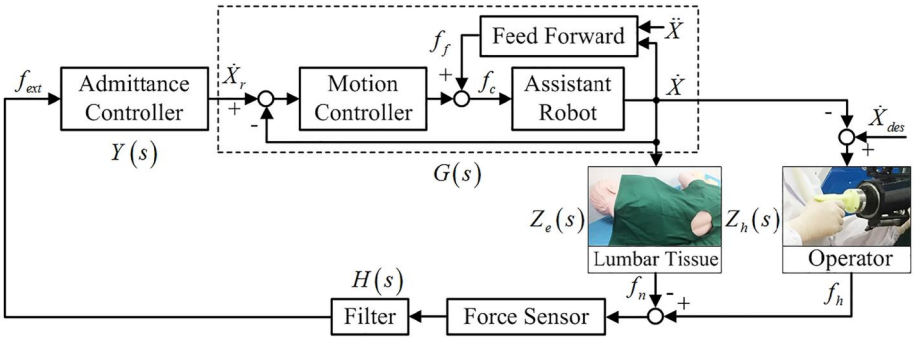

FIGURE 1 Control algorithm of the admittance control for the collaborative lumbar puncture robot system with underlying motion controller. The human operator's input force to the admittance controller provides the reference motion which is the lower level motion-controlled robot must follow

3.2.1 | Simplified admittance controller

The common type of admittance control is proportional to the velocity control,[29] where the admittance of the robot is reduced to a simple gain K_a, which makes the robot velocity output linearly proportional to the human applied force.

$$\dot{x}_r = K_a f_{ext} \tag{9}$$

where K_a is a constant admittance gain, and the control law theoretically behaves like a massless viscous damper. This simplified controller has been widely used on surgical robot systems, such as the Steady Hand Robot[1,30] and SHER.[2,5,31]

3.2.2 | Normal admittance controller

Typically, the normal admittance model implemented in the literature is of the form

$$m_d\left(\ddot{x}_r - \ddot{x}_0\right) + b_d(\dot{x}_r - \dot{x}_0) + k_d(x_r - x_0) = f_{ext} \tag{10}$$

where m_d, b_d, and k_d are positive constant values, which represents the desired mass, damping, and stiffness specified by the designer, respectively. Additionally, $\ddot{x}_0, \dot{x}_0$, and x_0 represent the equilibrium acceleration, velocity and position, respectively. $\ddot{x}_r, \dot{x}_r$, and x_r are the virtual desired acceleration, velocity, and trajectory obtained from the external applied force f_{ext}, respectively.

In specific situations, such as when the robot is guided by a human operator, the input to the robot system comes from the physical human robot interaction. A spring type effect is not preferred for collaborative tasks because it forces the robot end-effector to return to the equilibrium position. This condition is not desirable for robot-assisted lumbar puncture surgery. Consequently, the virtual desired stiffness k_d and virtual equilibrium position x_0 are set to zero. Finally, we aim at controlling the surgical robot to behave according to the following desired behaviour:

$$m_d\ddot{x}_r + b_d\dot{x}_r = f_{ext} \tag{11}$$

Taking the Laplace transform for the above equation, yields

$$\dot{X}_r(s) = \frac{F_{ext}(s)}{m_d s + b_d} \tag{12}$$

where $\dot{X}_r(s)$ and $F_{ext}(s)$ are Laplace transforms of $\dot{x}_r(t)$ and $f_{ext}(t)$, and s is the Laplace variable.

4 | STABILITY ANALYSIS

The surgical robot system should be stable in spite of the variation of the external environment, while helping the surgeon to achieve a high surgical task performance. The stability requirement is one of the key aspects of robotic applications, especially in the surgical manipulation domain, where it implies inherent safety for both the patient and surgeon.[32] The impedance variation both in the environment and human operator are the two main factors affecting the stability of the coupled system.

To express how well the robot-assisted lumbar puncture system performs, the sensitivity function $S(s)$ is defined as the metric of the system stability. This sensitivity function expresses the sensitivity of the closed human-robot coupled system to small perturbations of human environment dynamics.[33] For the lumbar puncture robotic control system shown in Figure 2, the sensitivity transfer function is defined as

$$S(s) = \frac{1}{L(s) + 1} \tag{13}$$

where $L(s) = G(s)Y(s)H(s)Z_{eq}(s)$ denotes the loop transfer function of the cooperation system, $G(s)$ is the linear time invariant model of the lumbar puncture robot, $Y(s)$ is the model of the admittance controller, $H(s)$ is the model of a low pass filter to attenuate the noise in external applied force measurements, and $Z_{eq}(s)$ models the equivalent impedance of the lumbar tissue and human operator. During the needle insertion operation, it is assumed that operator grasps the handle of the robot to guide the needle and puncture the patient's tissue. Consequently, the impedance of the human operator and objective environment are assumed to be coupled, which results in $Z_{eq}(s) = Z_h(s) + Z_e(s)$.

In spired by,[34] a cost function to quantify the system stability is defined as

$$\eta = \frac{1}{\max(|S(s)|)} \tag{14}$$

where $\max(|S(s)|)$ denotes the maximum magnitude of the loop sensitivity function of the lumbar puncture robotic system. The stability map used to characterise the stability of the collaborative lumbar puncture robot system for different controller parameters is shown by Figure 2. It is constructed to evaluate the effect of admittance parameters to changes in the equivalent human-tissue coupled impedance $Z_{eq}(s)$. The range of mass m_{eq}, damping b_{eq} and stiffness k_{eq} of the human arm used for the graphical representation of the stability are taken as $m_{eq} = 0 \sim 5$ kg, $b_{eq} = 0 \sim 41$ Ns/m, and $k_{eq} = 0 \sim 401$ N/m. As shown in Figure 2, as the system mass increases, the damping of the system should be increased to stabilise the cooperative surgical robot system.

5 | FORCE AMPLIFICATION ALGORITHM

5.1 | Impedance-filtered amplification algorithm

During the needle insertion operation, the displacement is decreased at the needle tip for safety consideration and increased manipulation precision. From the operator side, the puncture force between the

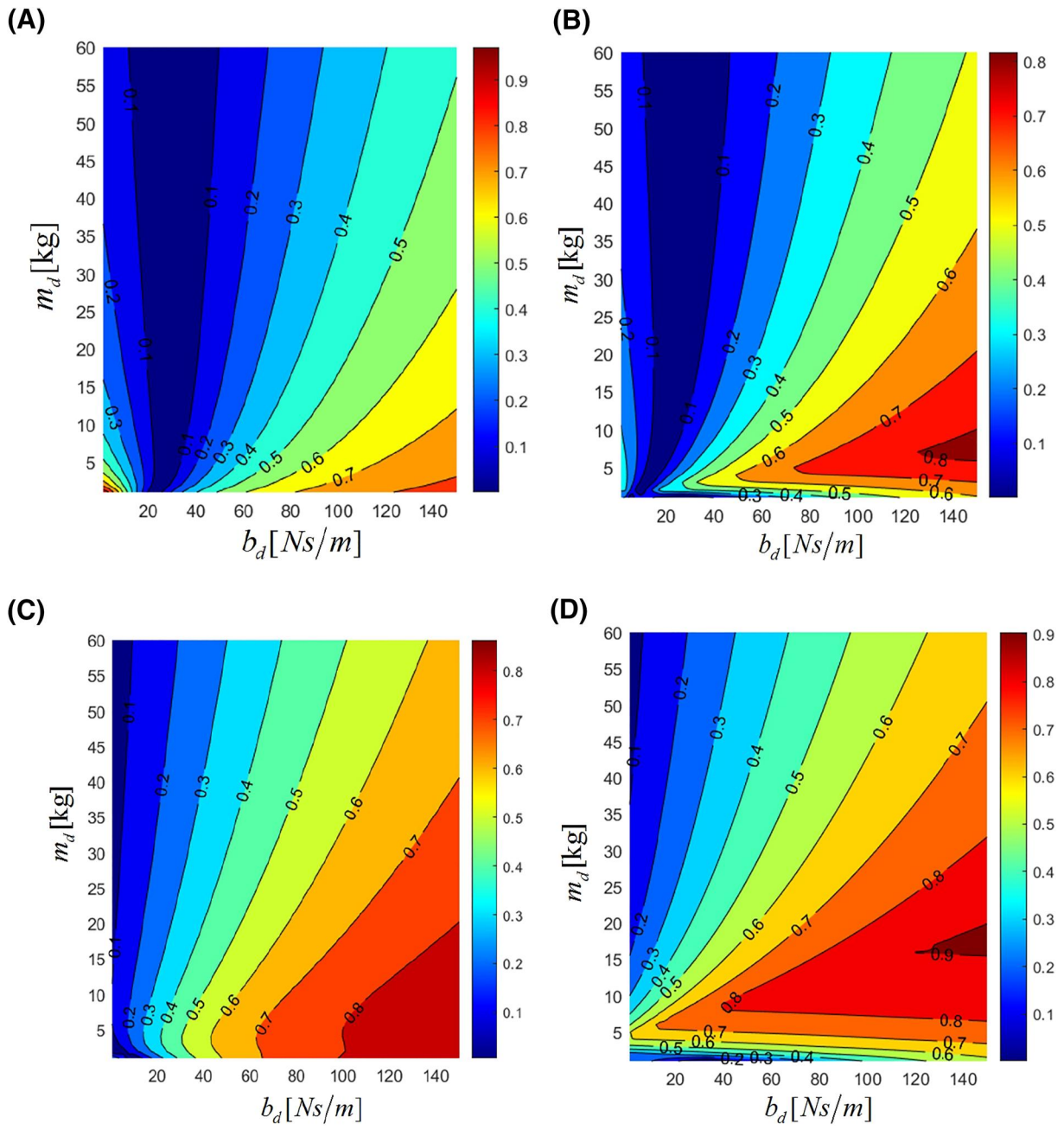

FIGURE 2 Stability map of the lumbar puncture robot system with different control parameters. (A) $m_{eq} = 0kg$, $b_{eq} = 0Ns/m$, $k_{eq} = 401\ N/m$,(B) $m_{eq} = 0\ kg$, $b_{eq} = 41Ns/m$, $k_{eq} = 401N/m$,(C) $m_{eq} = 5kg$, $b_{eq} = 0Ns/m$, $k_{eq} = 401N/m$, (D) $m_{eq} = 5kg$ $b_{eq} = 41Ns/m$ $k_{eq} = 401N/m$

needle and human tissue should be amplified and displayed to the surgeon.

From the control point of view, there are two types of solutions to satisfy the above requirements. The first one is the implicit force trajectory tracking controller which utilises the admittance with the error between the command and measured interaction forces. However, some practical problems should be addressed with the implementation of the implicit force trajectory tracking algorithm. One of the main problems that need to be resolved is the typically noisy force signals measured both from the handle and needle force sensors. The derivation and subtraction of the measured force signals are therefore not desirable, especially when the noisy needle interaction forces are amplified.

In this study, the impedance-filtered method[34] was implemented to set the desired needle position $x_r(t)$

$$x_r(t) = \int_0^t e_p(t)dt \tag{15}$$

where $e_p(t) = \alpha\dot{x}_h(t) - \beta\dot{x}_n(t)$ is the velocity tracking error between the amplified impedance-filtered human velocity and needle velocity, respectively. Additionally, α and β are constant positive gains to amplify the filtered desired velocities.

The noisy input force $f_h(t)$ applied by the human operator is filtered by the impedance regulator $Z_h(t)$, which transforms the noisy force signal into a clean desired velocity $\dot{x}_h(t)$.

The expression in the complex frequency domain is given by

$$\dot{X}_h(s) = \frac{F_h(s)}{Z_h(s)} \tag{16}$$

where $\dot{X}_h(s)$ and $F_h(s)$ are the Laplace transforms of $\dot{x}_h(t)$ and $f_h(t)$, and s is the Laplace variable.

Similarly, the desired velocity $\dot{x}_n(t)$ obtained from the filtered environment interaction force $f_n(t)$ in complex frequency domain is given by

$$\dot{X}_n(s) = \frac{F_n(s)}{Z_n(s)} \tag{17}$$

where $\dot{X}_n(s)$ and $F_n(s)$ are the Laplace transforms of $\dot{x}_n(t)$ and $f_n(t)$, and s is the Laplace variable.

5.2 | Model analysis

Considering a steady-state (constant desired velocity) motion, which is usually performed during lumbar puncture needle insertion procedures, the value of the velocity tracking error $e_p(t)$ is then equal to zero,

$$\alpha\dot{x}_h(t) - \beta\dot{x}_n(t) = 0 \tag{18}$$

The impedance regulators $Z_h(t)$ and $Z_n(t)$ are all in a form similar to Equation (11); both the impedance models have the same parameters behaving similarly in the operation process,

$$Z_i(s) = m_i s + b_i \tag{19}$$

where $i = h, n$ stands for the filter impedance on the operator and puncture needle side, respectively.

To achieve stable surgical manipulation, the impedance parameters in both the operator and needle tip sides should be as small as possible. The virtual damping parameter b_i plays a key role in the response magnitude of the steady state, and the ratio of the inertia over the damping m_i/b_i defines the surgical robot system response time. We know that the frequency range of voluntary human movements during cooperative surgical operations is approximately 2 Hz.[34] When the damping coefficient b_i is selected as a very small value, the inertia should also be as small as possible to keep the ratio m_i/b_i constant. Here, we assume the inertia is a very small value which can be neglected. Substituting Equation (19) into Equation (18), and setting the damping parameters are the same $b = b_h = b_n$, the following relationship can be obtained,

$$f_n(t) = \frac{\alpha}{\beta} f_h(t) \tag{20}$$

The forces applied to the lumbar puncture needle during the insertion operation is shown by Figure 3. The collaborative surgical robot system is equipped with two commercially available force sensors to detect the needle tip cutting force $f_n(t)$ and operator's guiding force $f_h(t)$. Considering the steady-state motion during the surgical operation again, it is possible to obtaining the force balance equation on the lumbar puncture needle, as shown in Figure 4.

6 | EXPERIMENT

6.1 | Experimental setup

The admittance controller proposed above was validated experimentally using the collaborative lumbar puncture robot system. The experimental setup is shown in Figure 5. It was a four degree of freedom robot developed at the Shanghai Jiao Tong University for medical application[25–28] For the experiments reported in this section, all the joints of the robot, except one degree of freedom of the handle-needle linear stage, were immobilised. The active linear joint was powered by an 18-V brushed dc motor (Model DCX22L GB KL, Maxon motor Inc.) which interfaced with individual controllers (ADS 50/5, Maxon Motor Inc.). The dc motor is connected through a planetary gearhead GPX22 A (5.3:1 reduction). The linear joint was equipped with an encoder (ENX16 EASY) with a resolution of 4000 counts per revolution resulting in a linear position resolution of 0.5 μm per encoder count. The control algorithm is developed using RT-Linux and is implemented on a real-time operating computer with a sampling time of 1 ms.

Because both the free space and constrained motions are very important during the needle insertion operation, the experiment

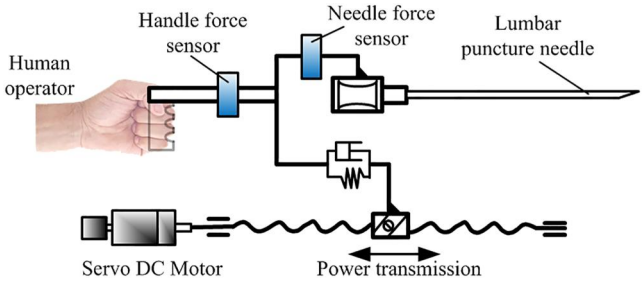

FIGURE 3 Overview of the lumbar puncture robot system. Two force sensors are used to sense the applied force by operator and external interaction force with tissue. A servo dc motor is utilised to drive the motion of the whole robotic system

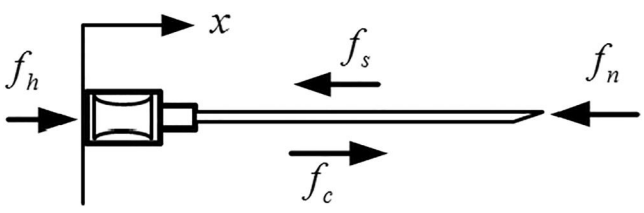

FIGURE 4 Forces simultaneously acting on the lumbar puncture needle

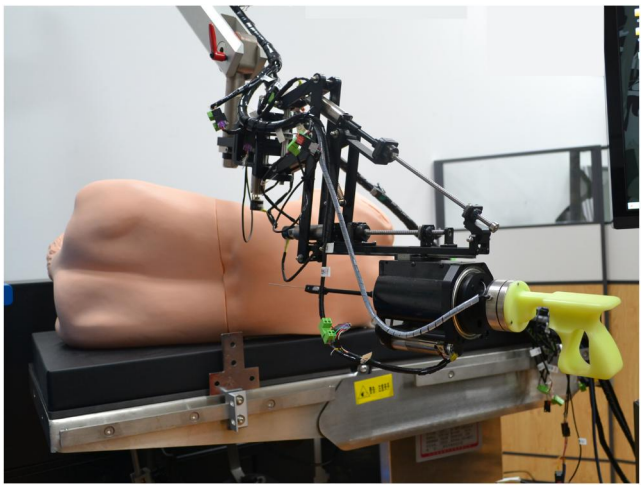

FIGURE 5 Setup of the lumbar puncture task on the phantom human tissue by collaborative surgical robot system

section of this study focuses on both the system performance of the free motion and constrained situation. The following two system properties will be verified in the collaborative lumbar puncture robotic system to ensure stable manipulation with low effort, namely: (*i*) position and velocity tracking performance of the needle tip during operation, (*ii*) scaled force tracking during the constrained motion. The motion and force tracking performance of the controller presented in this study will be validated with the experiments described in the following sections.

6.2 | Free motion tracking for low and high admittances

To assess the motion and force tracking performances of the lumbar puncture robot system, two tests were conducted with different sets of parameters, namely, desired damping and inertia. The first experiment consists of the pursuit of an approximately sinusoidal signal in free motion which is manually generated by a human operator with low admittance parameters. Figure 6 shows more details of the system response, such as the responding velocity and position, with low admittance parameters ($m_d = 0.002$ kg, and $b_d = 0.002$ Ns/m). The inner velocity-based servo controller, defined in (Equation 7), is implemented in the lumbar puncture robotic system. The stable position and velocity tracking performances are achieved. As shown by Figure 6B, the velocity has a small tracking error for the sub-level velocity controller. However, there is a relatively larger position tracking error between the desired position produced by the operator and the actual needle tip position, as shown in Figure 6A. The position and velocity tracking error between the output of the controller and needle tip output is shown in Figure 6C. From the experimental results, it can be clearly observed that the velocity tracking error is relatively smaller than the one in the position tracking as the only proportional velocity controller utilized in the robotic system.

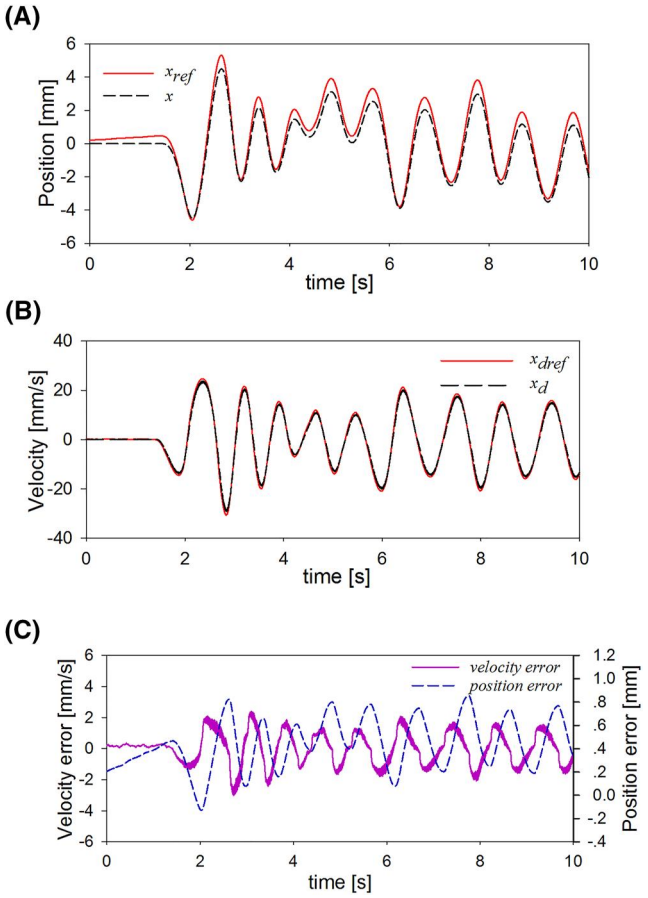

FIGURE 6 Experimental results of fast free motion using normal admittance control algorithm with lower level proportional velocity controller ($B = 0.002$ Ns/m, $M = 0.002$ kg). (A) position tracking with much more tracking error, (B) Velocity tracking with small tracking error, (C) Velocity and position tracking error

The second experiment was carried out with a high admittance situation under the same control parameters for the sub-level motion controller ($m_d = 0.01$ kg, and $b_d = 0.03$ Ns/m) under free motion. Figure 7 shows the details of the lumbar puncture robotic system response in the corresponding position and velocity tracking. With high admittance parameters, as shown in Figure 7A, the needle tip of the robotic system can follow the desired position of the admittance controller. As shown in Figure 7B,C, the increased admittance parameter results in an improvement of the velocity tracking accuracy. Therefore, it can be used to prove that the precision motion of the assisted robot can be effectively controlled with high the admittance parameters of the robot.

6.3 | Position-based vs velocity-based low level controller

The adaptation of the surgical robot to the operator characteristics is the necessary condition for a collaborative human-robot interaction with high transparency. The most commonly used method to satisfy this condition is the position-based admittance controller. However,

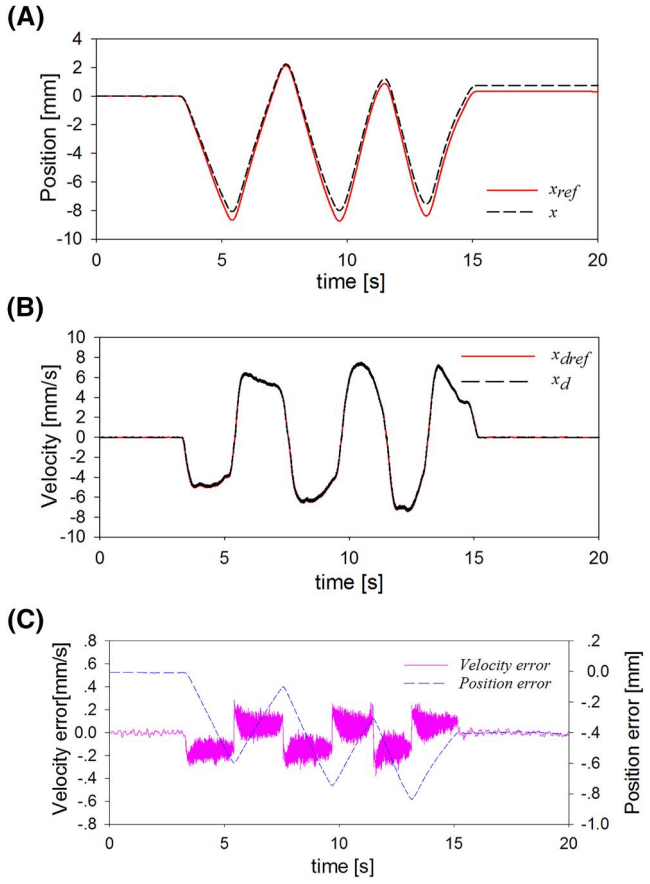

FIGURE 7 Experimental results of free motion using the normal admittance control algorithm with proportional velocity control (B = 0.03 Ns/m, M = 0.01 kg), (A) position tracking, (B) Velocity tracking, (C) Input force applied by human operator.

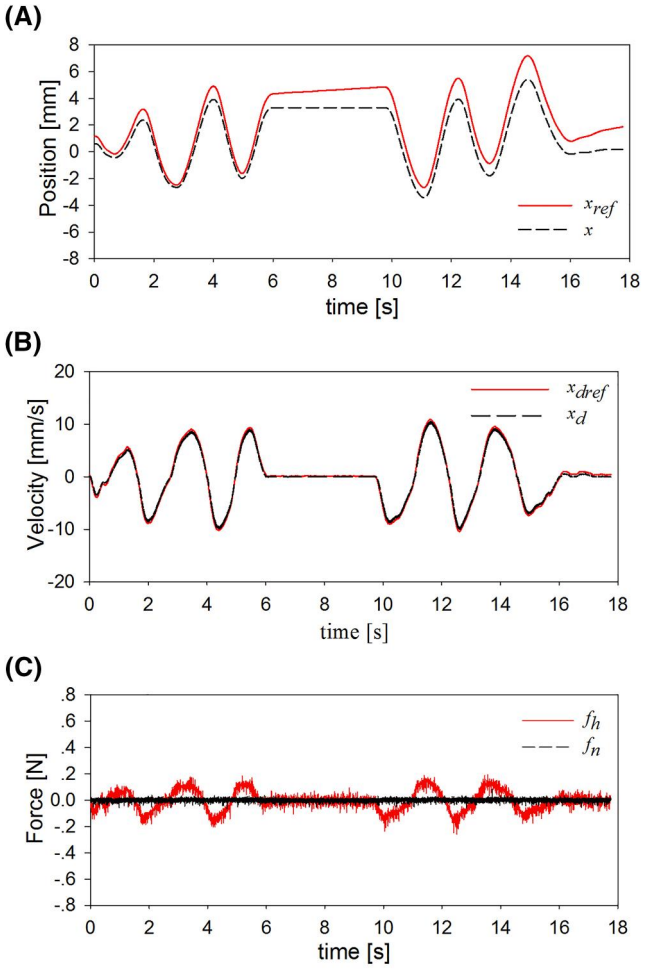

FIGURE 8 Experimental results of fast free motion using the normal admittance control algorithm with lower level proportional velocity controller (B = 0.012 Ns/m, M = 0.002 kg). (A) position tracking with large stable tracking error, (B) Velocity tracking with small tracking error, (C) Input force applied by human operator and the force applied to the robot end-effector

the admittance controller with the inner velocity motion control is also well known in the human-robot cooperation system. From the operator's manipulation feeling point of view, the actual difference between the two types of controller is negligible for the human-robot cooperation system with low joint friction. For the lumbar puncture robot system utilised in this study, which exhibits significant friction in its linear joints, the maneuverability of the robotic system should be verified by experiments. Figures 8 and 9 show the experimental results. The aim of this experiment was to determine the ability of the position and velocity-based admittance controllers to make the lumbar puncture robot behave according to a given set of desired admittance ($m_d = 0.002$ kg, and $b_d = 0.012$ Ns/m).

A human subject was asked to manipulate the handle of the surgical robot using the two different lower level motion controllers successively. The manipulation time was recorded from the starting moment to the stop movement, when the velocity of the needle tip was zero. The completion time for the manipulation task is the applied force from the operator exhibiting an inverse relationship because the high force reduces the time of a task with a relatively high velocity.

The position tracking performance of the two lower level motion controllers are shown in Figures 8A and 9A, respectively. Compared with the velocity-based admittance controller, a high position tracking performance is achieved for the system utilising position-based lower-level controller. The two sets of control methods obtained approximate experimental results in velocity tracking, as shown in Figures 8B and 9B. The responding applied forces on the robot handle by the operator are shown in Figures 8C and 9C, respectively. The mean applied force to the collaborative lumbar puncture robot is approximately 2N for both the position- and velocity-based low level controller. From the mean applied force, it can be concluded that the required human effort during the free needle manipulation is almost the same for both lower level controllers.

6.4 | Scaled interaction force tracking performance

The second experiment demonstrates how the collaborative robotic system behaves for a continuous interaction between the free and the constrained spaces. Firstly, the operator is asked to manipulate

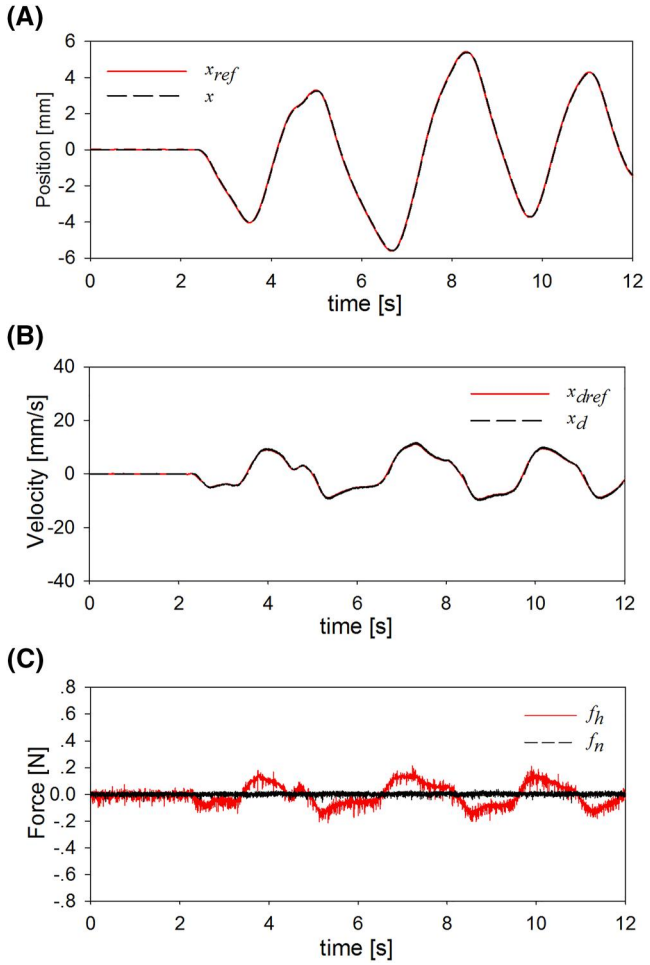

FIGURE 9 Experimental results of fast free motion using the normal admittance control algorithm with lower level PD controller (B = 0.012 Ns/m, M = 0.002 kg). (A) position tracking with good tracking results, (B) Velocity tracking with small tracking error, (C) Input force applied by human operator and the force applied to the robot end-effector

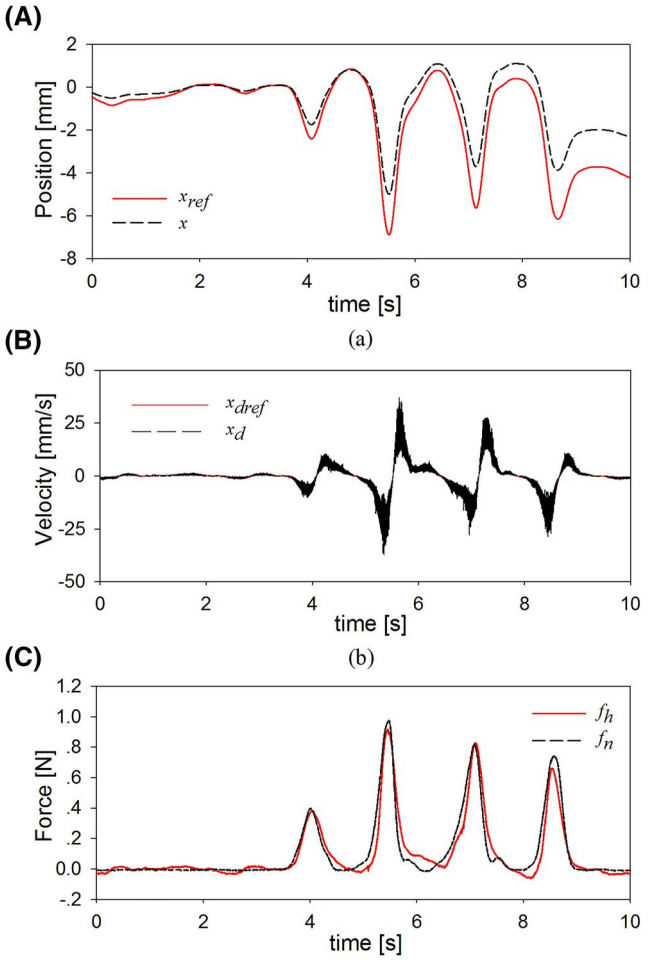

FIGURE 10 Experimental results of dynamic interaction with soft environment using force scaling admittance control algorithm. Lower level motion controller is proportional velocity control. (A) Position tracking with large stable tracking error, (B) Velocity tracking with small tracking error, (C) Input force applied by human operator and the force applied to the robot end-effector.

the robot end-effector in free space. And then the needle-environment dynamic interaction is introduced by pushing the needle to a compliant object. During such interaction period, the amplification to the needle interaction force is initiated, followed by a pull back to finally return to a displacement in free space again.

Figure 10 depicts the above mentioned situation with the default admittance parameters. In this experiment, the inner velocity-based controller by (Equation 7) is utilised. The desired and the response position of the lumbar puncture robot system is shown in Figure 10A. There is a relatively large position tracking error in between the desired position and the actual needle position for the lower level velocity-based controller. Velocity plots are shown in Figure 10B, and also there are some noisy signal in the actual response velocity of the surgical robot, an accurate tracking of the reference velocity resulting from the operator's guiding force is achieved. Moreover, the operator applied force input and the environment force response to the needle are represented in Figure 10C. A zero needle-environment interaction force is obtained in the free motion. On the contrary, a stable force tracking between the human operator $f_h(t)$ and the needle-environment interaction force $f_n(t)$ in the constrained mode is obtained.

6.5 | Applied force control of simplified admittance controller

The third experiment is carried out to obtain information specifically on the operator force control under the simplified admittance control law (9). Accurate surgical operation is an important goal of the surgical robot system design. This proportional-velocity control is the most common and simplest type of admittance control, where the admittance of the robotic system reduces to a simple admittance gain K_a. The experiment was performed by right-handed subjects using their right hand. The target force value (0.1 N) is provided to the subject on a computer screen place at a distance of 0.2 m by the operator. The force applied by operator is displayed on the screen

and the subject is instructed to match the target force and keep the applied force to the desired value to the best of her/his ability. The range of admittance gains K_a used in this experiment are 3, 6, 12, 20, and 30 mm/(Ns), respectively. The experimental results are shown in Figure 11. These figures show the typical force-versus-time and velocity-versus-time responses for a subject each at different values of the admittance gain K_a.

The results reported in Figure 11A,C,E,H,J indicate that the ability to control the applied force degrades as we increase the admittance gain K_a. In this study, we have presented compelling

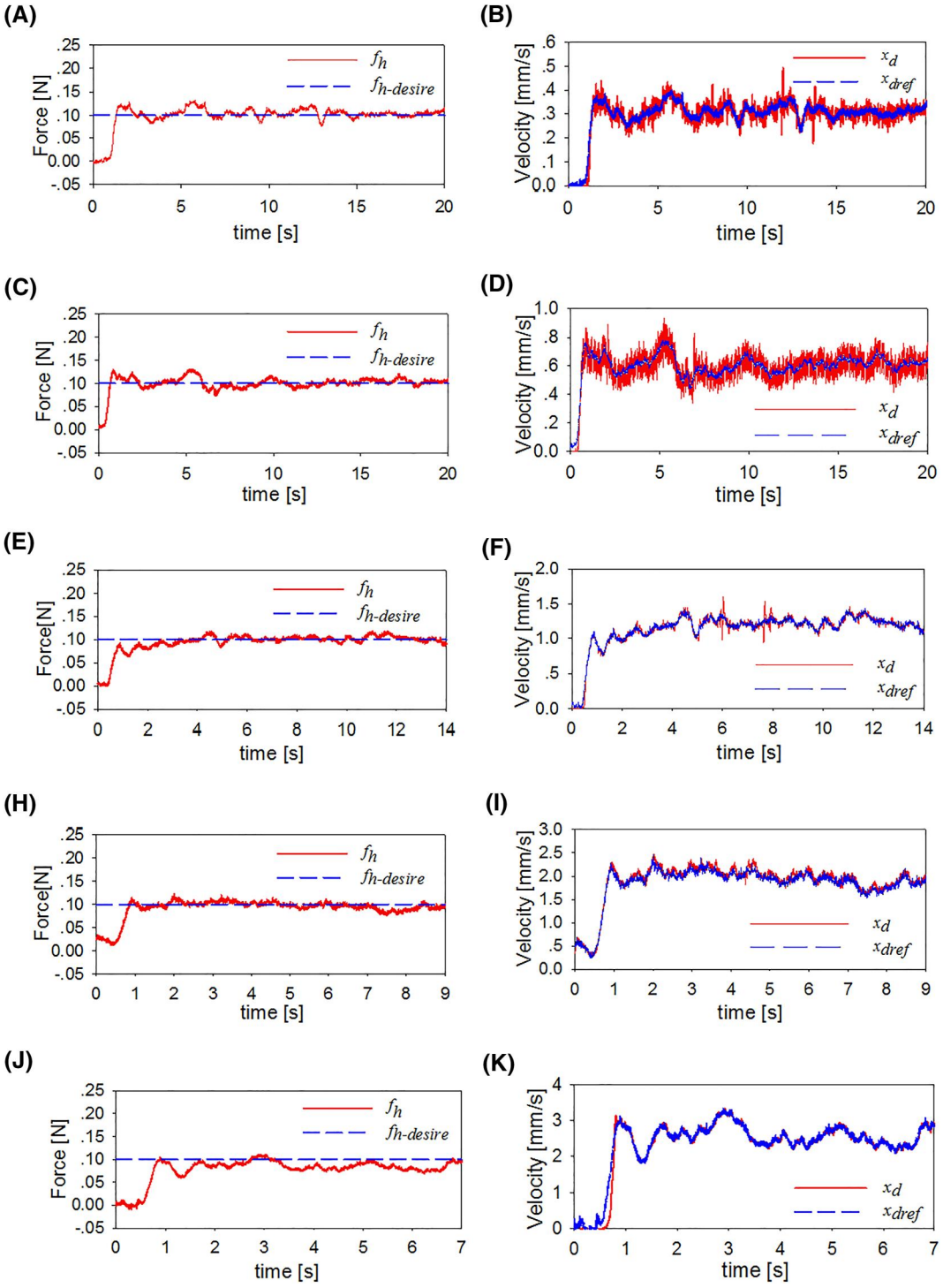

FIGURE 11 Experimental results of force and velocity tracking performance for simplified admittance controller with different level of admittance gain K_a. (A, B) force and velocity tracking with $K_a = 3$ mm/Ns, (C) and (D) force and velocity tracking with $K_a = 6$ mm/Ns, (E) and (F) force and velocity tracking with $K_a = 12$ mm/Ns, (H) and (I) force and velocity tracking with $K_a = 20$ mm/Ns, (J) and (K) force and velocity tracking with $K_a = 30$ mm/Ns

evidence that the admittance gain has a significant effect on the force control precision, which correlates with the observations presented by Nambi et al.[35] At higher values of the admittance gain, the force control precision decreases with the growing K_a.

The velocity tracking performance of the robotic system is shown in Figure 11B,D,F,I,K. The velocity of the system is increased with the augmentation of the admittance gain. When the admittance gain K_a is set as 3 and 6 mm/(Ns), a noticeable vibration is observed in the actual velocity signal. We observe that at $K_a = 20$ mm/Ns, the robotic system exhibits both precise force and velocity tracking performance. Based on the above experimental results, we could also conclude that, to obtain the best system performance for an admittance-type surgical robot, the admittance gain should be carefully selected to consider both the force tracking effect and speed tracking performance. Consequently, a tradeoff has to be reached between the applied force control accuracy and operator comfort.

7 | CONCLUSION AND FUTURE WORK

In this study, a preliminary feasibility study on the use of an enhanced position-based force-to-motion controller for cooperatively assisted surgical needle-insertion tasks on soft tissues was presented. We proposed an approach for the scaling of the needle-tissue interaction force to achieve force perception to human operators during needle insertion operations under a robotic needle assistant equipped with force sensors. The proposed admittance controller demonstrated comparable performance with respect to the state-of-the-art admittance schema. It was also shown experimentally that low-level position control is more appropriate than a simplified inner velocity-based admittance controller for the cooperative lumbar puncture surgical robot system. In comparison with the teleoperated surgical robot system, the proposed cooperative manipulation control scheme allows the operator to manipulate the same surgical tool that is performing the needle insertion surgery. We also established that there is a tradeoff between the human applied force precision and operator fatigue. Future work will focus on the evaluation of the force augmentation scheme with a pool of expert surgeons on a realistic lumbar phantom model to exploit the possibility of realizing safety features for the cooperative lumbar puncture robot.

ACKNOWLEDGEMENTS

This work was partially sponsored by the Projects of the Shanghai Science and Technology Committee under Grant 21S31906100, 22S31904100, and 21S31903300. The author Evgeni Magid acknowledges support of the Kazan Federal University Strategic Academic Leadership Program (PRIORITY-2030).

CONFLICT OF INTEREST

The authors have no conflict of interest to declare.

DATA AVAILABILITY STATEMENT

The data that support the findings of this study are available on request from the corresponding author.

ORCID

Hongbing Li https://orcid.org/0000-0003-2420-3104

REFERENCES

1. Roy J, Rothbaum DL, Whitcomb LL. Adaptive force control of position/velocity controlled robots: theory and experiment. *IEEE Trans Robot Autom*. 2002;18(2):121-137.
2. Zhou M, Wu J, Ebrahimi A, et al. Spotlight-based 3D instrument guidance for autonomous task in robot-assisted retinal surgery. *IEEE Rob Autom Lett*. 2021;6(4):7750-7757.
3. Saeidi H, Opfermann JD, Kam M, et al. Autonomous robotic laparoscopic surgery for intestinal anastomosis. *Sci Robot*. 2022;7(62):1-13.
4. Wu G, Podolsky D, Looi T, Kahrs LA, Drake JM, Forrest CR. A 3 mm wristed instrument for the da Vinci robot: setup, characterization, and phantom tests for cleft palate repair. *IEEE Trans Med Robot Bionics*. 2020;2(2):130-139.
5. Ebrahimi A, Urias MG, Patel N, et al. Adaptive control improves sclera force safety in robot-assisted eye surgery: a clinical study. *IEEE (Inst Electr Electron Eng) Trans Biomed Eng*. 2021;68(11):3356-3365.
6. Kastritsi T, Doulgeri Z. A controller to impose a RCM for hands-on robotic-assisted minimally invasive surgery. *IEEE Trans Med Robot Bionics*. 2021;3(2):392-401.
7. Yohannes P, Rotariu P, Pinto P, et al. Comparison of robotic versus laparoscopic skills: is there a difference in the learning curve? *Adult Urol*. 2002;60(1):39-45.
8. Leijte E, Blaauw I, Workum F, et al. Robot assisted versus laparoscopic suturing learning curve in a simulated setting. *Surg Endosc*. 2020;34:3679-3689.
9. Enayati N, Momi E, Ferrigno G. Haptics in robot-assisted surgery: challenges and benefits. *IEEE Rev Biomed Eng*. 2016;9:49-65.
10. He X, Balicki M, Gehlbach P, et al. A Multi-Function Force Sensing Instrument for Variable Admittance Robot Control in Retinal Microsurgery. *IEEE International Conference on Robotics and Automation (ICRA)*; 2014.
11. Osa T, Uchida S, Sugita N, Mitsuishi M. Hybrid rate admittance control with force reflection for safe teleoperated surgery. *IEEE/ASME Trans Mechatron*. 2015;20(5):2379-2390.
12. Bae J, Kim K, Huh J, Hong A. Variable admittance control with virtual stiffness guidance for human-robot collaboration. *IEEE Access*. 2020;8:117335-117346.
13. Bazzi D, Roveda F, Zanchettin A, Rocco P. A unified approach for virtual fixtures and goal-driven variable admittance control in manual guidance applications. *IEEE Rob Autom Lett*. 2021;6(4):6378-6385.
14. Keemink A, Kooij H, Stienen A. Admittance control for physical human-robot interaction. *Int J Robot Res*. 2018;37(11):1421-1444.
15. Ferraguti F, Landi C, Sbattini L, et al. A variable admittance control strategy for stable physical human-robot interactions. *Int J Robotics Res*. 2019;38(6):747-765.
16. Ficuciello F, Villani L, Siciliano B. Variable impedance control of redundant manipulators for intuitive human-robot physical interaction. *IEEE Trans Robot*. 2015;31(4):850-863.
17. Dimeas F, Aspragathos N. Online stability in human-robot cooperation with admittance control. *IEEE Trans Haptics*. 2016;9(2):267-278.

18. Landi C, Ferraguti F, Sabattini L, et al. Admittance control parameter adaptation for physical human-robot interaction. *IEEE Int Conf Robot Autom (ICRA)*. 2017:2911-2916.
19. Sharkawy A, Koustournpardis P, Aspragathos N. Variable admittance control for human-robot collaboration based on online neural network training. *IEEE/RSJ Int Conf Intelligent Robots Syst (IROS)*, 2018: 1334-1339.
20. Aydin Y, Tokatli O, Patoglu V, Basdogan C. Stable physical human-robot interaction using fractional order admittance control. *IEEE Trans Haptics*. 2018;11(3):464-475.
21. Kang G, Oh HS, Seo JK, et al. Variable admittance control of robot manipulators based on human intention. *IEEE/ASME Trans Mechatron*. 2019;24(3):1023-1032.
22. Bazzi D, Lapertosa M, Zanchettin A, Rocco P. Goal-driven Variable Admittance Control for Robot Manual Guidance. *IEEE/RSJ International Conference on Intelligent Robots and Systems (IROS)*, pp. 9759-9766. 2020.
23. Duchaine V, Gosselin CM. General Model of Human-Robot Cooperation Using a Novel Velocity Based Variable Impedance Control. *Second Joint EuroHaptics Conference and Symposium on Haptic Interfaces for Virtual Environment and Teleoperator Systems*. WHC, pp. 446-451, 2007.
24. Lorenzo D, Koseke Y, Momi E, et al. Coaxial needle insertion assistant with enhanced force feedback. *IEEE (Inst Electr Electron Eng) Trans Biomed Eng*. 2013;60(2):379-389.
25. Li H, Wang Y, Li Y, Zhang J. A novel manipulator with needle insertion forces feedback for robot-assisted lumbar puncture. *Int J Med Robot Comput Assist Surg*. 2021;17(2):1-11.
26. Wang Y, Li H. Penetration detection with intention recognition for cooperatively controlled robotic needle insertion. *Trans Inst Meas Control*. 2022;44(10):1979-1992.
27. Wang Y, Zhang J, Li H, Penetration identification criterion and augmentation for pediatric lumbar puncture. *IEEE International Conference on Robotics and Biomimetics (ROBIO)*, Sanya, pp. 267-271, 2021.
28. Li Y, Zhang J, Gui D, Li H, Enhanced epidural tissue perception for pediatric patients by an interactive lumbar puncture simulator. *IEEE International Conference on Robotics and Biomimetics (ROBIO)*, Sanya, pp. 1767-1772, 2021.
29. Arbuckle T, Nambi M, Butner J, et al. Human velocity control of admittance-type robotic devices with scaled visual feedback of device motion. *IEEE Trans Human-Mach Syst*. 2016;46(6):859-868.
30. Kumar R, Berkelman P, Gupta P, et al. Preliminary experiments in cooperative human/robot force control for robot assisted microsurgical manipulation. *IEEE Int Conf Robot Autom (ICRA)*. 2000;1:610-617.
31. Ebrahimi A, He C, Patel N, et al. Sclera force control in robot-assisted eye surgery: Adaptive force control vs. Auditory feedback. *International Symposium on Medical Robotics (ISMR)*; 2019.
32. Srikar A, Kumar P, Thondiyath A, et al. Enhancement of stability and transparency in teleoperated robots through isotropy-based design. *IEEE Access*. 2020;8:17273-17286.
33. Åström KJ, Murray RM. *Feedback Systems: An Introduction for Scientists and Engineers*. Princeton University Press; 2010.
34. Aydin Y, Tokatli O, Patoglu V, Basdogan C. A computational multicriteria optimization approach to controller design for physical human-robot interaction. *IEEE Trans Robot*. 2020;36(6):1791-1804.
35. Nambi M, Provancher WR, Abbott JJ. On the ability of humans to apply controlled forces to admittance-type devices. *Adv Robot*. 2011;25(5):629-650.

How to cite this article: Li H, Nie X, Duan D, et al. An admittance-controlled amplified force tracking scheme for collaborative lumbar puncture surgical robot system. *Int J Med Robot*. 2022;e2428. https://doi.org/10.1002/rcs.2428